# SPATIALLY VARYING RIEMANNIAN ELASTICITY REGULARIZATION: APPLICATION TO THORACIC CT REGISTRATION IN IMAGE-GUIDED RADIOTHERAPY

*T. Bjerre*[⋆†] *M.O. Fogtmann*[⋆] *M. Aznar*[†] *P. Munck af Rosenschöld*[†] *L. Specht*[†◇] *R. Larsen*[⋆]

[⋆] Department of Informatics and Mathematical Modelling, Image Analysis & Computer Graphics, Technical University of Denmark, Denmark.
[†] Department of Radiation Oncology, Rigshospitalet, Copenhagen University, Denmark.
[◇] Department of Oncology, Rigshospitalet, Copenhagen University, Denmark.

## ABSTRACT

For deformable registration of computed tomography (CT) scans in image guided radiation therapy (IGRT) we apply Riemannian elasticity regularization. We explore the use of spatially varying elasticity parameters to encourage bone rigidity and local tissue volume change only in the gross tumor volume (GTV) and the lungs. We evaluate the method on the point-validated 4DCT breathing thorax POPI-model and demonstrate its use and properties in registration of pre- and post-chemo CT scans for contour propagation in a Hodgkin lymphoma (HL) case showing significant tumor shrinkage. For the POPI-model we achieved a total mean target registration error (TRE) of $0.92 \pm 0.49$ mm. Using spatially varying regularization for the HL case, deformation was limited to the GTV and lungs.

## 1. INTRODUCTION

In IGRT, dose distribution is planned based on manual contouring of the tumor and critical normal tissues on a pre-treatment positron emission tomography - computed tomography (PET-CT) scan. Conventional radiation therapy (RT) treatment is fractionated; patients receive a daily fraction of the total planned dose. Throughout the course of treatment, spatial changes of the patient may cause residual positional errors even after translational and rotational image guided corrections. Such changes include tumor shrinkage [4, 1], weight loss, organ filling and change in posture, all of which cause tissue deformation, ultimately disturbing the planned dose distribution. Hansen et al. [6] concluded that adaptive replanning is essential for intensity-modulated radiation therapy (IMRT) treatment for head & neck (H&N) cancer to ensure proper dose to target volumes and critical tissues.

Manual tumor re-contouring on a daily basis is unfeasible due to the massive amount of physician time and effort required. Adaptive RT techniques allow for automatic, but preferably supervised, correction of these spatial changes on a daily basis. Contours of the GTV and critical tissues can be propagated by use of image registration, and the dose distribution can be updated accordingly.

Image registration is the process of determining a spatial transformation that establishes meaningful correspondence between all points in a pair or set of images; in this case between the planning PET-CT and a subsequent CT or cone-beam CT (CBCT) scan. In general, image registration comprises 3 main aspects. **1**. Selecting an image transformation model, $T$. **2**. Selecting an objective function $\mathcal{F}_{obj}$, including an image (dis)similarity measure $\mathcal{D}$ and a regularization term $\mathcal{R}$ ensuring a plausible, invertible transformation. **3**. Selecting an optimization strategy for the objective function.

Here, we explore the use of the Riemannian elasticity model for regularization, proposed by Pennec et al. [11]. Based on a Hounsfield units (HU) threshold segmentation, Ruan et al. [12] applied spatially varying regularization encouraging bone rigidity and Kabus et al. [9] used spatially varying elasticity. In a similar fashion, we use spatially varying tissue regularization parameters, enabling us to encourage local rigidity and volume change. Specifically, we seek to exploit the a priori knowledge that volume change is likely to happen in the GTV.

We evaluate spatially varying Riemannian elasticity regularization on the POPI-model, a point-validated 4DCT breathing thorax data set, and further illustrate its use on a HL case with pre- and post-chemotherapy CT scans.

## 2. DATA

### 2.1. POPI-model: 4DCT

The POPI-model is a point-validated 4DCT image data set of a breathing thorax. The dataset was acquired at the Lon Brard Cancer Center & CREATIS lab, Lyon, France. It is available at `http://www.creatis.insa-lyon.fr/rio/popi-model` and is described by Vandemeulebroucke et al. [17]. The data set consists of ten volume images, each in a different phase of one breathing cycle. The images are cropped to volumes of $482 \times 360 \times 141$ voxels at a resolution of $0.98 \times 0.98 \times 2.0$ mm, including only the thorax. Forty

landmarks have been manually annotated in each of the images. Performance is evaluated by calculating the TRE as the euclidean distance between the points annotated in the target scan and the deformed points from the reference scan (first phase). For images downsampled to a resolution of $2 \times 2 \times 2$ mm, a mean TRE for all scans of $1.24 \pm 0.42$ was achieved using a non-parametric Demons method from Sarrut et al. [15], inspired by Thirion [16]. A mean TRE of $1.04 \pm 0.53$ mm was achieved using a parametric, multi-scale implementation by Delhay et al. [3] of the free-form deformation (FFD) deformation model by Rueckert et al. [13]. Glocker et al. [5] reports a mean TRE of $0.96 \pm 0.57$ mm (on the downsampled data) using a discrete graph-based, multi-scale FFD method.

### 2.2. Hodgkin lymphoma case: Pre- and post-chemo CT

A HL patient with a very large mediastinal tumor burden was staged with a fluorodeoxyglucose (FDG) PET-CT scan before the initiation of chemotherapy. Later, the patient was referred to RT, where a planning CT scan was acquired. In HL, the RT target volume is the PET-positive volume as it was defined on the staging (pre-chemotherapy) scan. However, between the staging and planning scan, the tumour burden is likely to have been reduced considerably, the patient is likely to have lost weight and the posture is likely to vary. Automatic deformable registration and propagation of the PET-positive contour to the RT planning CT would be a valuable aid to the physician, when defining the radiation target volume.

## 3. METHOD

We applied a sum-of-squared-differences (SSD) driven FFD B-spline model [13] to register the staging and planning CT scans allowing for a subsequent mapping of the GTV contour to the planning CT. The use of the cubic B-spline deformation model is motivated partly by the existence of direct analytic continuous derivatives and partly by the inherent dimensionality reduction. We believe that the B-spline deformation model has enough descriptive power to capture the *true* underlying deformations between the scans as we are estimating the mapping between images of the same subject. In a multi-level framework, an L-BFGS [10] algorithm was applied to solve the matching problem, i.e.

$$\min_{\phi} \mathcal{D}(R, T \circ \phi) + \mathcal{R}(\phi), \tag{1}$$

where $\mathcal{D}$ is the SSD (di)similarity measure, $R$ is the reference (staging CT), $T$ is the target (planning CT), $\phi$ is the B-spline transformation and $\mathcal{R}$ is the regularization term.

Biological studies, e.g. [8, 14], show that biological tissue is similar to rubber; nearly incompressible and compliant to shear. Thus a rubber-like deformation prior is suitable for same-subject registration when images are acquired temporally close. However, cancer patients are likely to have significant weight loss, have tumor shrinkage and tissue loss in proximity to the tumor regions which makes the incompressibility constraint invalid. Relaxing the incompressibility constraint transforms the rubber prior into a more general elasticity prior.

Linear elasticity matching [2] has been widely used for spatial normalization but the lack of local rotation invariance can hinder optimal matching. Especially in H&N imaging, the neck posture (bending in the neck) may cause the linear elasticity prior to over-regularize the deformation. We applied an *isotropic* Riemannian elasticity prior by Pennec et al. [11], with spatially varying elasticity parameters as a trade-off between modelling capability and simplicity. The Riemannian elasticity prior is a *simple* weighted quadratic penalty on the Hencky strain tensor which inherits local rotational invariance and the *infinity* energy limit approaches the *black-hole* deformation. While biological tissue is elastically anisotropic, anisotropic modeling requires many parameters which cannot be estimated from CT scans alone. Instead, isotropic behaviour is assumed, reducing the number of parameters to two – namely the usual Lamé parameters $\mu, \lambda$, giving the isotropic Riemannian elasticity

$$\mathcal{R}_{rie}(\mu, \lambda; \phi) = \frac{\mu}{4} \sum_{i=1}^{N} \log^2 \varepsilon_i + \frac{\lambda}{8} \left( \sum_{i=1}^{N} \log \varepsilon_i \right)^2, \tag{2}$$

where $\mu$ controls the amount of elastic potential due to shearing, and $\lambda$ controls the amount of elastic potential due to local compression or expansion. $\varepsilon_i$ are the principal stretches. In contrast to linear elasticity and Saint-Vernant Kirchoff elasticity $\lambda$ is solely related to local volume change [7]. The Lamé parameters are set experimentally for each tissue type (bone, soft tissue, lung) which are segmented from the planning CT using HU intensity thresholding. In addition, the Lamé parameters are set *low* in the GTV to allow for considerable shrinkage. The image maps of Lamé parameters are smoothed to get smooth elastic potential transitions.

## 4. RESULTS

### 4.1. POPI-model

For the FFD transformation model, Glocker et al. [5] used multi-level control point spacing of $40, 20, 10, 5$ mm. We have used two registration levels with 20 and 10 mm spacing. Additional registration levels did not improve performance. Level 1 used downsampling to $4 \times 4 \times 4$ mm and level 2 used downsampling to $2 \times 2 \times 2$ mm. Table 1 presents the registration results using both spatially constant and varying regularization. For spatially varying regularization, the provided segmentation of the lung was used together with a HU-based bone segmentation for assigning local Lamé regularization parameters. Rigidity was encouraged only for bone, by setting $\mu_{\text{bone}} \gg \mu_{\text{soft tissue}}, \mu_{\text{lung}}$. Volume change was encouraged only for lung by setting $\lambda_{\text{lung}} \ll \lambda_{\text{soft tissue}}, \lambda_{\text{bone}}$.

**Table 1**. POPI-model registration results

| # | Initial mean distance [mm] | mean TRE [mm] (spatially constant) | mean TRE [mm] (spatially varying) |
|---|---|---|---|
| 1 | $0.48 \pm 0.54$ | $0.65 \pm 0.33$ | $0.64 \pm 0.31$ |
| 2 | $0.49 \pm 0.62$ | $0.65 \pm 0.42$ | $0.63 \pm 0.39$ |
| 3 | $2.19 \pm 1.84$ | $1.19 \pm 0.68$ | $1.19 \pm 0.70$ |
| 4 | $4.33 \pm 2.54$ | $1.01 \pm 0.50$ | $1.02 \pm 0.50$ |
| 5 | $5.75 \pm 2.67$ | $1.08 \pm 0.62$ | $1.08 \pm 0.63$ |
| 6 | $6.10 \pm 2.96$ | $0.98 \pm 0.53$ | $1.00 \pm 0.54$ |
| 7 | $5.03 \pm 2.36$ | $1.08 \pm 0.50$ | $1.09 \pm 0.53$ |
| 8 | $3.68 \pm 1.59$ | $0.80 \pm 0.40$ | $0.77 \pm 0.41$ |
| 9 | $2.07 \pm 1.07$ | $0.84 \pm 0.42$ | $0.82 \pm 0.43$ |
| All | $3.35 \pm 2.82$ | $0.92 \pm 0.49$ | $0.92 \pm 0.49$ |

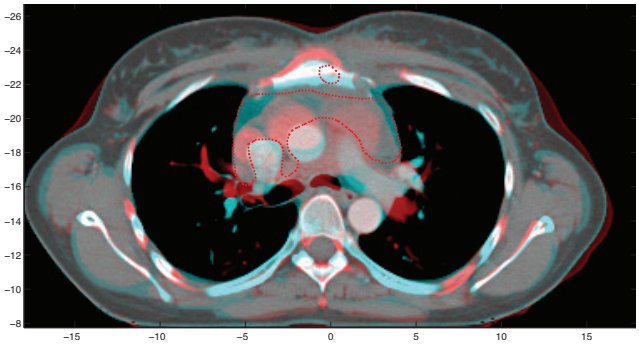
### 4.2. Pre- and post-chemo CT

For spatially varying regularization, triangulation-based GTV segmentation and HU-based segmentation of bone, soft tissue and lung was used for assigning local Lamé regularization parameters. Rigidity was encouraged only for bone, by setting $\mu_{\text{bone}} \gg \mu_{\text{soft tissue}}$. Volume change was encouraged for both GTV and lung by setting $\lambda_{\text{GTV}}, \lambda_{\text{lung}} \ll \lambda_{\text{soft tissue}}, \lambda_{\text{bone}}$.

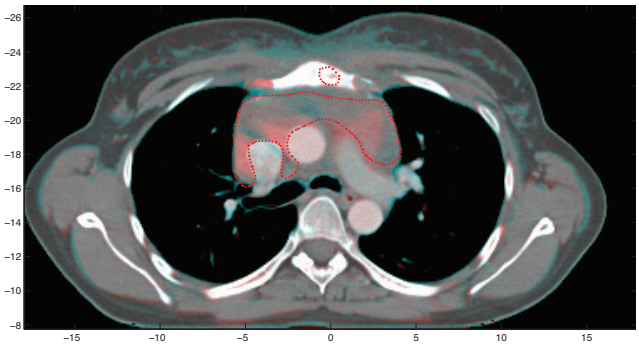
Figure 1 displays a fusion of a single transverse slice of the pre-chemo CT and the deformed post-chemo CT. Figure 2 shows the Jacobian determinant of the transformation field, i.e. the local volume change, in the same slice. The initial tumor volume was $140\text{cm}^2$. Using spatially constant regularization, the volume of the propagated contour was $120\text{cm}^2$. Using spatially varying regularization, the volume of the propagated contour was $99\text{cm}^2$. Comparing segmentations from the propagated contours to a manual post-chemo GTV segmentation resulted in Dice similarity coefficients of $0.43$ in both cases versus $0.39$ using rigid registration.

## 5. DISCUSSION & CONCLUSION

For the POPI-model we achieved a total mean TRE smaller than what has been reported in the literature. The standard deviation is also small. For the breathing phases with low initial mean distance, deformation resulted in a mean TRE larger than the initial distance. This was expected as the registration was based on downsampled images. The standard deviation, however, was significantly decreased in these cases. There was no difference between the results obtained using spatially constant and varying regularization, most likely due to the ab-

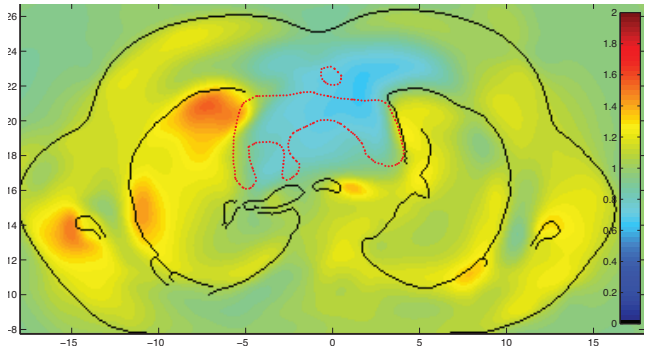


Spatially constant regularization

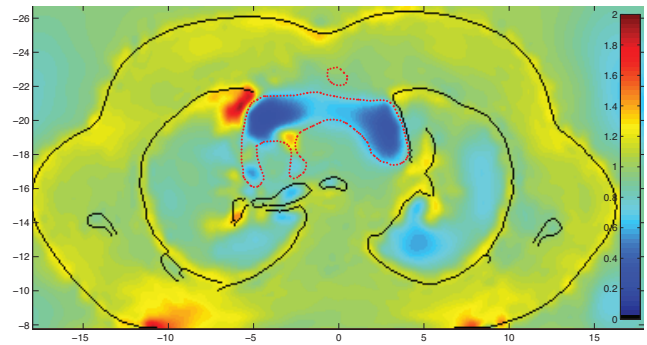


Spatially varying regularization

**Fig. 1**. Overlay of transverse slice of pre-chemo CT and deformed post-chemo CT. The red, dotted line is the PET-positive contour.



Spatially constant regularization



Spatially varying regularization

**Fig. 2**. Volume change in the transverse slice in 1. Values of 1 indicate no local volume change. The black contour is gradients extracted from the CT.

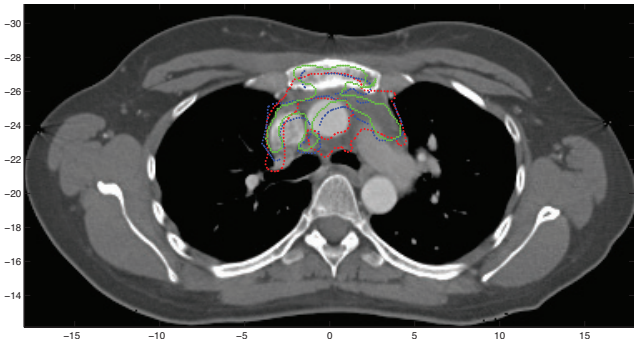



**Fig. 3**. Post-chemo CT with manually propagated and adapted contour (red) and contours propagated automatically using spatially constant (blue) and varying (green) regularization.

sence of significant volume changes. In that respect, this data set is not troublesome. For the HL case we demonstrated that local volume change can be encouraged in volumes where it is expected (GTV, lungs, etc.). The Dice similarity coefficients between the manual post-chemo GTV segmentation and those based on deformable registration were relatively low, primarily due to the clinician choosing to include a larger area on the planning scan. Still, the coefficients were higher than that of the rigid registration, suggesting that this would be a better starting point for the clinician who is manually propagating and modifying the contour. By visual inspection it is apparent that qualitatively, the registration result using spatially varying regularization is superior. The method could very well be suitable for registration to low-quality scans with deranged image gradients, in order to minimize local volume change, e.g. CBCT scans for daily contour propagation in adaptive RT. As with all parametric image registration methods, the main drawback is parameter optimization. In this regard, the use of spatially varying regularization parameters is a further encumbrance.

# References

[1] J. L. Barker et al., "Quantification of volumetric and geometric changes occurring during fractionated radiotherapy for head-and-neck cancer using an integrated CT/linear accelerator system," *International Journal of Radiation Oncology Biology Physics*, vol. 59, no. 4, pp. 960–970, Jul. 2004.

[2] C. Broit, "Optimal registration of deformed images," PhD thesis, University of Pennsylvania, 1981.

[3] B. Delhay et al., "Locally adapted spatio-temporal deformation model for dense motion estimation in periodic cardiac image sequences," *Functional Imaging and Modeling of the Heart*, pp. 393–402, 2007.

[4] S. Erridge et al., "Portal imaging to assess set-up errors, tumor motion and tumor shrinkage during conformal radiotherapy of non-small cell lung cancer," *Radiotherapy and oncology*, vol. 66, no. 1, pp. 75–85, 2003.

[5] B. Glocker et al., "Deformable Medical Image Registration : Setting the State of the Art with Discrete Methods," *Annual Review of Biomedical Engineering*, no. 13, pp. 219–244, 2011.

[6] E. K. Hansen et al., "Repeat CT imaging and replanning during the course of IMRT for head-and-neck cancer.," *International journal of radiation oncology, biology, physics*, vol. 64, no. 2, pp. 355–62, Feb. 2006.

[7] M. F. Hansen, "The Virtual Knife," PhD thesis, Technical University of Denmark, 2009.

[8] T. Hu, "Reality-based soft tissue probing: experiments and computational model for application to minimally invasive surgery," PhD thesis, Drexel University, 2006.

[9] S. Kabus et al., "Spatially varying elasticity in image registration.," *Methods of information in medicine*, vol. 46, no. 3, pp. 287–91, Jan. 2007.

[10] D. Liu et al., "On the limited memory BFGS method for large scale optimization," *Mathematical programming*, vol. 45, no. 1, pp. 503–528, 1989.

[11] X Pennec et al., "Riemannian elasticity: a statistical regularization framework for non-linear registration.," *MICCAI 2005*, vol. 8, no. Pt 2, pp. 943–50, Jan. 2005.

[12] D. Ruan et al., "Nonrigid registration using regularization that accomodates local tissue rigidity," *Proceedings of SPIE*, vol. 6144, pp. 614 412–614 4129–, 2006.

[13] D Rueckert et al., "Nonrigid registration using free-form deformations: application to breast MR images.," *IEEE transactions on medical imaging*, vol. 18, no. 8, pp. 712–21, Aug. 1999.

[14] P. Sarma et al., "Non-linear material models for tracheal smooth muscle tissue," *Bio-medical materials and engineering*, vol. 13, no. 3, p. 235, Jan. 2003.

[15] D. Sarrut et al., "Simulation of four-dimensional CT images from deformable registration between inhale and exhale breath-hold CT scans," *Medical Physics*, vol. 33, no. 3, p. 605, 2006.

[16] J.-P. Thirion, "Image matching as a diffusion process: an analogy with Maxwell's demons," *Medical image analysis*, vol. 2, no. 3, pp. 243–260, Sep. 1998.

[17] J. Vandemeulebroucke et al., "The POPI-model, a point-validated pixel-based breathing thorax model," in *ICCR 2007*, 2007, pp. 1–8.